PCP
PLANT & CELL PHYSIOLOGY

Octaketide Synthase from *Polygonum cuspidatum* Implements Emodin Biosynthesis in *Arabidopsis thaliana*

Yanwu Guo[1,2,4], Sara Nassar[3], Lanqing Ma[2,5], Guanping Feng[1,2,6], Xing Li[1,2], Mo Chen[1], Tuanyao Chai[1], Iman A. M. Abdel-Rahman[3,7], Till Beuerle [3], Ludger Beerhues [3], Hong Wang [1,2,*] and Benye Liu [3,*]

[1]College of Life Sciences, University of the Chinese Academy of Sciences, Beijing 100049, China
[2]Institute of Botany, The Chinese Academy of Sciences, Beijing 100093, China
[3]Institute of Pharmaceutical Biology, Technische Universität Braunschweig, Mendelssohnstrasse 1, Braunschweig 38106, Germany
[4]Present address: Department of Biosciences, University of Oslo, Blindernveien 31, Oslo 0371, Norway.
[5]Present address: College of Bioscience and Resources Environment, Beijing University of Agriculture.
[6]Present address: School of Life Sciences, Jinggangshan University, Ji'an 343009, China.
[7]Present address: Department of Pharmacognosy, Faculty of Pharmacy, South Valley University, Qena 83523, Egypt.
*Corresponding authors: Hong Wang, E-mail, hwang@ucas.ac.cn; Fax, +86-10-6967-2644; Benye Liu, E-mail, b.liu@tu-bs.de; Fax, +49-531-391-8104.
(Received 16 September 2020; Accepted 18 October 2020)

Regular Paper

Plant anthranoids are medicinally used for their purgative properties. Their scaffold was believed to be formed by octaketide synthase (OKS), a member of the superfamily of type III polyketide synthase (PKS) enzymes. Here, a cDNA encoding OKS of *Polygonum cuspidatum* was isolated using a homology-based cloning strategy. When produced in *Escherichia coli*, *P. cuspidatum* octaketide synthase (PcOKS) catalyzed the condensation of eight molecules of malonyl-CoA to yield a mixture of unphysiologically folded aromatic octaketides. However, when the ORF for PcOKS was expressed in *Arabidopsis thaliana*, the anthranoid emodin was detected in the roots of transgenic lines. No emodin was found in the roots of wild-type *A. thaliana*. This result indicated that OKS is the key enzyme of plant anthranoids biosynthesis. In addition, the root growth of the transgenic *A. thaliana* lines was inhibited to an extent that resembled the inhibitory effect of exogenous emodin on the root growth of wild-type *A. thaliana*. Immunochemical studies of *P. cuspidatum* plants detected PcOKS mainly in roots and rhizome, in which anthranoids accumulate. Co-incubation of *E. coli*-produced PcOKS and cell-free extract of wild-type *A. thaliana* roots did not form a new product, suggesting an alternative, physiological folding of PcOKS and its possible interaction with additional factors needed for anthranoids assembling in transgenic *A. thaliana*. Thus, transgenic *A. thaliana* plants producing PcOKS provide an interesting system for elucidating the route of plant anthranoid biosynthesis.

Keywords: Anthranoids • *Arabidopsis thaliana* • Emodin • Octaketide synthase • *Polygonum cuspidatum* • Type III polyketide synthase.

Accession numbers: The nucleotide sequences reported in this article have been submitted to Genbank under accession numbers: **PcOKS gene**, **MN708050**, **PcOKS ORF**, **EU647244**.

Introduction

Plant anthranoids comprise anthrones, anthraquinones and dianthrones, which are used as laxatives, and naphthodianthrones (hypericins), which are developed for photodynamic diagnosis and therapy (Dewick 2009, Ritz et al. 2012). Biosynthesis of anthranoids in plants is proposed to be catalyzed by octaketide synthase (OKS), which belongs to the superfamily of type III polyketide synthase (PKS) enzymes. PKSs produce a large variety of polyketide scaffolds, such as chalcone, stilbene, acridone, curcumin and isocoumarin (Schröder 1997, Austin and Noel 2003). All known type III PKSs are homodimers with a subunit molecular mass of 40–45 kDa. They catalyze the iterative condensation of acetyl units from the decarboxylation of malonyl-CoA to a starter CoA ester in a biosynthetic process that closely parallels fatty acid biosynthesis. The functional diversity of type III PKSs is due to the differences in the selection of the starter molecules, the number of the malonyl-CoA condensations and the mechanisms of cyclization reactions (Austin and Noel 2003, Abe and Morita 2010). Despite the remarkable functional diversity, type III PKSs of plant origin usually share a 50–75% amino acid sequence identity with each other.

The starter for OKS is acetyl-CoA, which is stepwise condensed with seven molecules of malonyl-CoA to form a linear octaketide intermediate (**Fig. 1**; Abdel-Rahman et al. 2013). It was proposed that under in vivo conditions the linear octaketide intermediate is converted to emodin anthrone via atrochrysone by three aldol-type condensations and dehydration (Dewick, 2009). Oxidation of the central cyclohexadienone ring in emodin anthrone yields emodin, which can be methylated to physcion. Genes encoding OKSs from *Aloe arborescens* and *Hypericum perforatum* have been cloned and functionally characterized (Abe et al. 2005a, Karppinen et al. 2008, Mizuuchi et al. 2009). Both recombinant enzymes formed a linear octaketide, which, however, was incorrectly cyclized to give the two

Plant Cell Physiol. 62(3): 424–435 (2021) doi:10.1093/pcp/pcaa135, Advance Access publication on 4 February 2021, available online at https://academic.oup.com/pcp

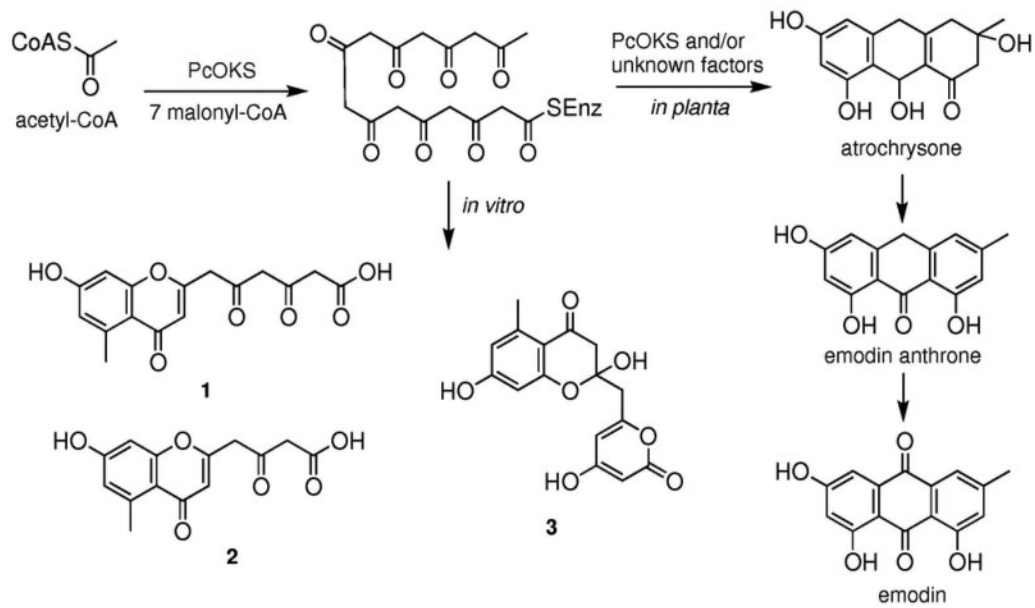

Fig. 1 Schematic illustration of reactions catalyzed by PcOKS in vitro and in planta. **1**, 6-(7-hydroxy-5-methyl-4-oxo-4*H*-chromen-2-yl)-3,5-dioxohexanoic acid; **2**, 4-(7-hydroxy-5-methyl-4-oxo-4*H*-chromen-2-yl)-3-oxobutanoic acid; **3**, SEK4b.

aromatic polyketides SEK4 and SEK4b rather than atrochrysone. Thus, both PKSs were incapable of accomplishing the proposed in vivo reaction under in vitro conditions, raising the question of whether an additional factor or enzyme may be involved in plant anthranoid biosynthesis. A polyketide cyclase that functions cooperatively with a tetraketide synthase in cannabinoid biosynthesis was identified in *Cannabis sativa* (Gagne et al. 2012).

Polygonum cuspidatum Sieb. et Zucc. (Polygonaceae), commonly known as Japanese knotweed in English and Huzhang in Chinese, is a herbaceous perennial medicinal plant, which is widely distributed in eastern Asia countries, such as China, Japan and Korea. The roots of *P. cuspidatum* have been used for centuries as an important traditional Chinese medicine for dispelling wind-evil, eliminating damp, alleviating pain, relieving cough and reducing sputum (Zhang et al. 2013). Since 1977, the dried root of *P. cuspidatum* has been listed in the Pharmacopoeia of the People's Republic of China under the name 'Hu Zhang' (Editorial Committee of Chinese Pharmacopoeia 1977). In contrast to its medicinal uses in eastern Asia, *P. cuspidatum* is regarded as an invasive plant in Europe and North America due to its aggressive growth, allelopathic effect and extremely strong abiotic stress tolerance (Murrell et al. 2011, Dommanget et al. 2016). Pharmacological investigations demonstrated that extracts of *P. cuspidatum* have many activities, such as antioxidant, anticancer, hepatoprotective, cardioprotective, antiviral, antibacterial and antifungal properties (Jayasuriya et al. 1992, Xiao et al. 2002, Zhang et al. 2013, Peng et al. 2013). Extensive phytochemical investigations led to the isolation and identification of 67 compounds, including anthranoids, stilbenes, flavonoids, coumarins and lignans, from roots and leaves of *P. cuspidatum*, which provide chemical evidence for the pharmacological activities (Vastano et al. 2000, Xiao et al. 2002, Shan et al. 2008). The most abundant anthranoids isolated from *P. cuspidatum* are the anthraquinones emodin and physcion, which have potential antimicrobial and anticancer applications (Jayasuriya et al. 1992, Olsen et al. 2007, Gao et al. 2017). The major stilbenes are polydatin and resveratrol, which possess antimicrobial, anti-inflammatory, anti-HIV, cardioprotective and anticancer properties (Zhang et al. 2019). Emodin and polydatin are used as the indicator compounds to characterize the quality of plant material with minimum contents of 0.6% and 0.15%, respectively, in the Pharmacopoeia of the People's Republic of China (Editorial Committee of Chinese Pharmacopoeia 2015).

Polygonum cuspidatum transcripts encoding PKSs responsible for the biosynthesis of stilbenes and flavonoids were previously cloned and characterized in our laboratory (Ma et al. 2009a, Ma et al. 2009b, Guo et al. 2013). However, the *OKS* gene underlying the biosynthesis of anthranoids has not yet been isolated. In the present study, a transcript for an octaketide-producing enzyme of *P. cuspidatum* [*P. cuspidatum* octaketide synthase (PcOKS)] was isolated using a homology-based cloning strategy. For functional characterization, it was expressed in *Escherichia coli* and *Arabidopsis thaliana*. Detection of emodin in transgenic *A. thaliana* lines indicates that PcOKS is involved in anthranoid biosynthesis.

Results

Homology-based cloning yields the PcOKS cDNA

To isolate cDNAs encoding new PKSs of *P. cuspidatum*, RT-PCR was carried out using degenerate oligonucleotide primers (**Supplementary Table S1**) based on conserved regions of known plant PKSs and total RNA from roots of *P. cuspidatum* plantlets as a template with PCR program 1 (**Supplementary Table S2**). Five cDNA fragments with the expected size were

obtained, which included a 641-bp core cDNA fragment for PcOKS and four previously reported PKS sequences (Ma et al. 2009a, Ma et al. 2009b, Guo et al. 2013). The full-length cDNA for PcOKS was obtained using an RACE approach with PCR program 2 (**Supplementary Table S2**). The sequence data have been submitted to the GenBank databases under accession number EU647244. The open reading frame (ORF) of the PcOKS cDNA consisted of 1,176 bp and encoded a protein of 391 amino acids with a calculated molecular mass of 43.3 kDa and an isoelectric point of 6.2. The gene for PcOKS was amplified using genomic DNA as template and gene-specific primers derived from the ORF of the PcOKS cDNA. The sequence data have been submitted to the GenBank databases under accession number MN708050. *PcOKS* had a size of 1,449 bp and contained a single 273-bp intervening sequence, which is inserted between the first and second nucleotides of the Cys60 triplet (MsCHS2 numbering, **Supplementary Fig. S1**). This intron is conserved in all known PKS genes (Schröder 1997, Austin and Noel 2003). No significant homology was found between the intron of *PcOKS* and the introns of the other four *PcPKS* genes isolated previously.

Sequence analysis reveals structural characteristics of PcOKS

Multiple sequence alignment was performed using ClustalW2 with default parameters to compare PcOKS with a number of PKSs with similar functions as well as chalcone synthase 2 from *Medicago sativa* (MsCHS2, Ferrer et al. 1999). Although PcOKS shares only 53.5% and 47.4% amino acid sequence identity with *A. arborescens* octaketide synthase (AaOKS) and *H. perforatum* octaketide synthase (HpOKS), respectively, all three enzymes have an identical catalytic triad consisting of Cys164, His303 and Asn336 (MsCHS2 numbering) (**Fig. 2**). This triad is absolutely conserved in all type III PKSs of plant and bacterial origin (Ferrer et al. 1999, Austin et al. 2004). Furthermore, the majority of the CHS active site residues, including Met137, Gly211, Gly216 and Pro375, as well as the CHS gatekeepers Phe215 and Phe265 (MsCHS2 numbering) are conserved in PcOKS (**Fig. 2**).

However, three CHS active site residues lining the initiation/elongation cavity, Thr197, Gly256 and Ser338, are uniquely replaced in PcOKS with Ala, Leu and Thr, respectively. The same replacements are found in heptaketide-producing ALS from *Rheum palmatum* (Abe et al. 2004) and hexaketide-producing HKS from *Plumbago indica* (Springob et al. 2007). By contrast, the three amino acids are substituted by Gly, Leu and Val in AaOKS and by Ser, Gly and Trp in HpOKS. HKS from *Drosophyllum lusitanicum* contains Phe, Leu and Thr (Jindaprasert et al. 2008) and PCS from *A. arborescens* has Met, Leu and Val (Abe et al. 2005b). The characteristic three-amino-acid insertion 'PPE' located 10 residues upstream of the catalytic His303 of *A. arborescens* PKSs is absent from PcOKS and reduced to only one 'D' in HpOKS (Abe et al. 2005a, Karppinen et al. 2008). Homology modeling predicted that PcOKS has the same three-dimensional overall fold as MsCHS2 with a cavity volume of 1,470 Å^3. This volume is similar to those of AaOKS (1,685 Å^3) and HpOKS (1,611 Å^3) but larger than those of *R. palmatum* aloesone synthase (RpALS) (1,034 Å^3) and *A. arborescens* aloesone synthase (AaALS) (1,065 Å^3), which resemble that of MsCHS2 (1,019 Å^3). The comparison of the cavity sizes suggested that the active site of PcOKS is large enough to perform the seven successive condensation reactions and to accommodate the resulting octaketide product.

Phylogenetic analysis groups PcOKS with hexa- and heptaketide synthases

To further study the relationships between PcOKS and other type III PKSs, a phylogenetic analysis was performed using 71 function-known plant type III PKSs, including the four published PKSs from *P. cuspidatum* (**Fig. 3**). In the phylogenetic tree, PKSs from angiosperms were separated into two main clusters, CHSs and functionally divergent CHS-like enzymes. Interestingly, functionally similar CHS-like enzymes from different plants commonly grouped together, e.g. STSs from *P. cuspidatum* (PcSTS) and *Rheum tataricum* and BASs from *P. cuspidatum* and *R. palmatum*. The functionally characterized AaOKS clustered together with pentaketide synthase [*A. arborescens* pentaketide chromone synthase (AaPCS)] and heptaketide synthase (AaALS) from the same plant. Similarly, PcOKS was present in the cluster of CHS-like enzymes from angiosperms and appeared to be most closely related to the heptaketide-producing ALS from *R. palmatum* (Abe et al. 2004) and the hexaketide-producing hexaketide synthase (HKS) from *P. indica* (Springob et al. 2007). This observation suggested that PcOKS functionally resembles these latter two PKSs and may be able to catalyze either five or six condensation steps on a short starter to form hexaketide and heptaketide products, respectively.

PcOKS catalyzes octaketide synthesis in vitro

To identify the catalytic function of PcOKS in vitro, the ORF of the PcOKS cDNA was functionally expressed in the *E. coli* strain BL21-Rosetta (DE3) using the pET-30a (+) vector. The recombinant PcOKS protein contained an additional hexahistidine tag at its C-terminus, allowing its purification on Ni-NTA agarose to a high purity, as indicated by the presence of a single protein band in SDS-PAGE (**Supplementary Fig. S2**). The relative subunit molecular mass of the purified protein was approximately 45 kDa.

In assays with acetyl-CoA and [2-^{14}C]malonyl-CoA, at least seven products were detected when analyzed by HPLC coupled to a radiodetector (**Fig. 4A**). After further optimization of the assay conditions, two main products with RT values of 23.67 min (**1**) and 25.09 min (**3**) and one minor product with the RT value of 24.20 min (**2**) were detected (**Fig. 4B**). These products were absent in control assays containing heat-denatured enzyme, indicating their enzyme-dependent formation. The products were isolated and further analyzed by electrospray-ionization-mass spectrometry (ESI-MS). Both main products had the total mass of an octaketide (*m/z* $[M-H]^-$ 317) but underwent different fragmentations. Product **3** had two fragment ions under ESI$^-$ conditions at *m/z* 191 and 125, respectively, which were identical to those of SEK4b (**Fig. 4C;** Karppinen et al. 2008). Product **1** had five

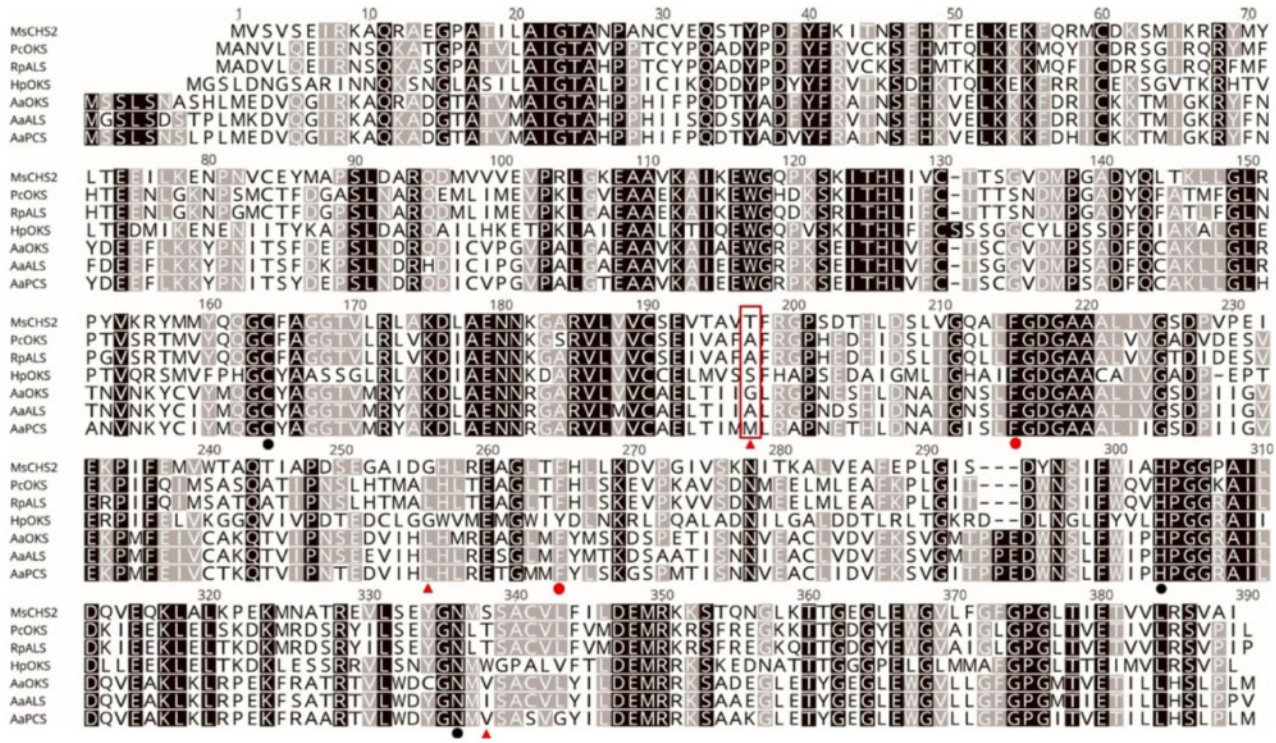

Fig. 2 Comparison of deduced amino acid sequences of *Polygonum cuspidatum* OKS and other plant-specific type III PKSs. Multiple sequence alignment was performed by ClustalW2 with default parameters. Black and gray backgrounds indicate identical and consensus amino acids, respectively. The catalytic triad residues conserved in type III PKSs (Cys164, His303 and Asn336; MsCHS2 numbering) are marked with black dots. The residues lining the active site (Thr197, Gly256 and Ser338) are marked with red triangles. The 'gatekeeper' phenylalanines, Phe215 and Phe265, are marked with red dots. Thr197, which is crucial for controlling the polyketide chain length in different PKSs from *A. arborescens*, is labeled with a red box. Plant type III PKS sequences used: MsCHS2 (P30074); HpOKS (ACF37207); AaPCS (AAX35541); AaOKS (AAT48709); AaALS (AXN70004); *RpALS* (AAS87170); and PcOKS (ACC76752).

fragment ions under ESI^- conditions at *m/z* 273 (loss of CO_2), *m/z* 231 (loss of CH_3CO from fragment ion 273), *m/z* 189 (loss of CH_3CO from fragment ion 231), *m/z* 151 (loss of C_5H_3OH from fragment ion 231) and *m/z* 125 (loss of $C_6H_2O_2$) (**Fig. 4C**). Product **2** had a total mass of a heptaketide (*m/z* $[M-H]^-$ 275) with four fragment ions at *m/z* 231, 189, 151 and 125, which were identical to the last four fragment ions of product **1** (**Fig. 4C**, **Supplementary Fig. S3**). In addition, product **1** was partially converted to product **3** (SEK4b) with increasing incubation time (**Supplementary Fig. S4**). These data strongly suggested that product **1** was the octaketide 6-(7-hydroxy-5-methyl-4-oxo-4*H*-chromen-2-yl)-3,5-dioxohexanoic acid and product **2** was the heptaketide 4-(7-hydroxy-5-methyl-4-oxo-4*H*-chromen-2-yl)-3-oxobutanoic acid (**Figs. 1, 4B**). Thus, PcOKS appears to be OKS. The enzyme was able to utilize malonyl-CoA as the only substrate, which functions as both starter and extender to form the observed product profile. Therefore, it was impossible to determine the *K*m for acetyl-CoA. The *K*m for malonyl-CoA was 79.9 ± 19.5 μM ($n = 5$). The pH and temperature optima were 7 and 45°C, respectively.

In PKSs from *A. arborescens*, the amino acid at position 197 (MsCHS2 numbering) solely determines polyketide chain length and product specificity. The G197A mutant of AaOKS showed heptaketide synthase activity (Abe et al. 2005a, Abe et al. 2006). In PcOKS, the position 197 is alanine, however, the mutant enzyme A197G did not change the product profile (**Supplementary Fig. S5**). In HpOKS, this position is serine (Karppinen et al. 2008).

PcOKS implements emodin biosynthesis in *Arabidopsis thaliana*

To investigate the function of PcOKS in planta, the ORF of the PcOKS cDNA was transferred to *A. thaliana* via *Agrobacterium*-mediated transformation and it was expressed under the control of the CaMV 35S promoter. Immunoblotting after SDS-PAGE was used to detect the PcOKS protein in *A. thaliana*. An antiserum had been raised in rabbits against the His_6-PcOKS protein, which was produced in *E. coli*, and the IgG fraction was isolated by affinity chromatography. Immunoblotting indicated that (i) the IgG fraction specifically recognized PcOKS and (ii) the PcOKS ORF was expressed in three transgenic *A. thaliana* lines (**Fig. 5**).

To examine the functionality of PcOKS in *A. thaliana*, the metabolites present in various organs were extracted and analyzed by High-Performance Liquid Chromatography with Diode-Array Detection (HPLC-DAD). The anthranoid emodin

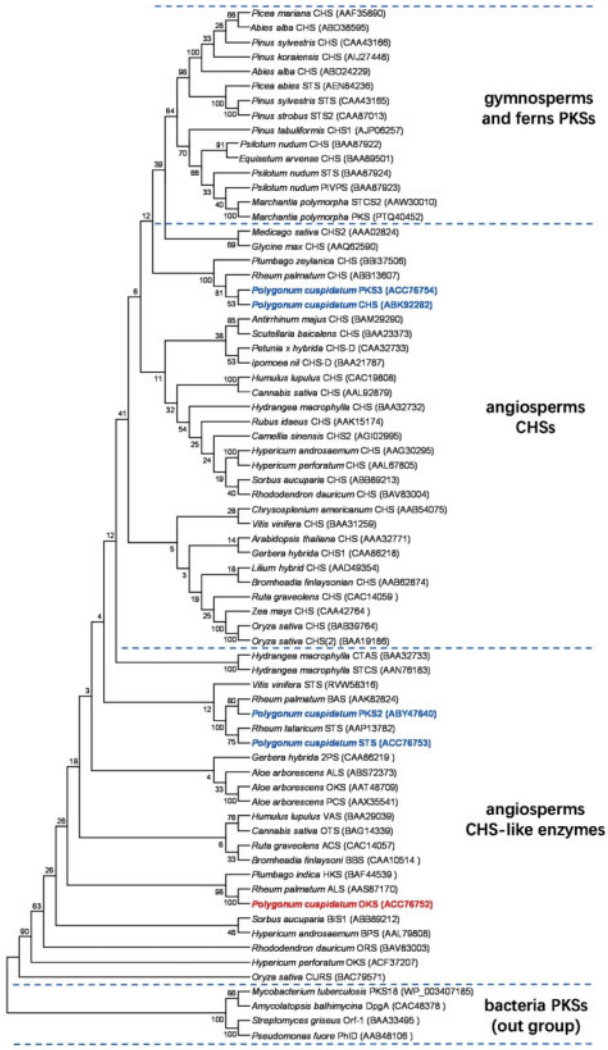

Fig. 3 Neighbor-joining tree of plant type III PKSs constructed using MEGA7 (Saitou and Nei 1987, Kumar et al. 2016). The percentages of replicate trees, in which the associated taxa clustered together in the bootstrap test (500 replicates), are indicated next to the branches (Felsenstein 1985). The evolutionary distances were computed using the Dayhoff matrix-based method (Schwarz and Dayhoff 1979). A total of 474 positions were present in the final dataset. The four bacterial type III PKSs served as outgroup to root the tree.

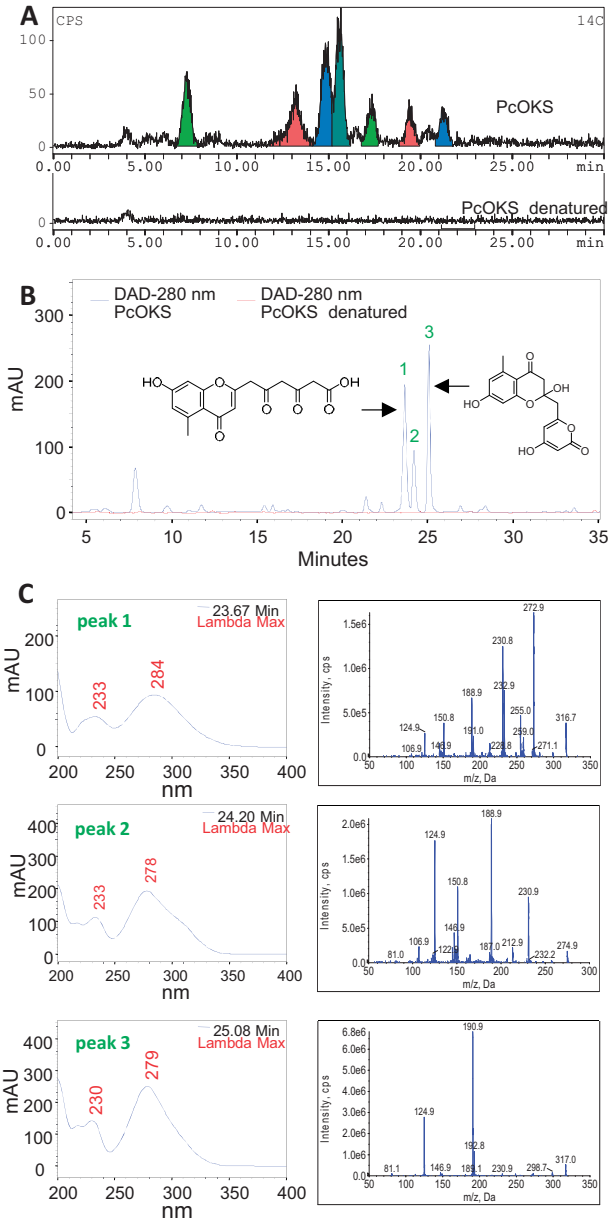

Fig. 4 Detection of enzymatic activity of affinity-purified PcOKS overexpressed in *E. coli* strain BL21-Rosetta (DE3). (A) Analysis of an enzyme assay containing [2-^{14}C]malonyl-CoA by HPLC coupled to a radiodetector; (B) analysis of a modified enzyme assay containing non-radioactive malonyl-CoA by HPLC-DAD; and (C) UV and electrospray-ionization-tandem mass spectrometry (ESI-MS/MS) spectra of the three main products indicated in (B).

was detected in the roots of three *A. thaliana* lines expressing the PcOKS ORF. Its identity was verified by ESI-MS in comparison to authentic emodin (**Fig. 6A, C**, **Supplementary Fig. S9**). The average emodin level among the three transgenic lines was 0.37 ± 0.26 mg g^{-1} dry weight (**Supplementary Table S3**). No traces of emodin were detected in the roots of wild-type *A. thaliana* (**Fig. 6B**), nor was emodin found in the shoots of transgenic *A. thaliana* (**Supplementary Fig. S9**, **Supplementary Table S3**).

Expression of the PcOKS ORF significantly inhibited the growth of the roots of transgenic *A. thaliana* lines (**Fig. 7A**). The average root length of lines that expressed *35S-PcOKS* was only 30% of that of wild-type plants (**Fig. 7B**). To investigate whether inhibition of the root growth in transgenic plants was caused by emodin, *A. thaliana* seeds were germinated on 1/2 Murashige and Skoog (MS) medium containing various concentrations of emodin (1–1,000 μg l^{-1}). At a concentration as low as 1 μg l^{-1}, emodin already exerted a significant inhibitory effect on the root growth of *A. thaliana* seedlings (**Supplementary Fig. S6A**). Emodin at 1,000 μg l^{-1} strongly inhibited the growth of both roots and shoots (**Supplementary Fig. S6B**). The average length of *A. thaliana* roots at this concentration was only 31% of the length of roots

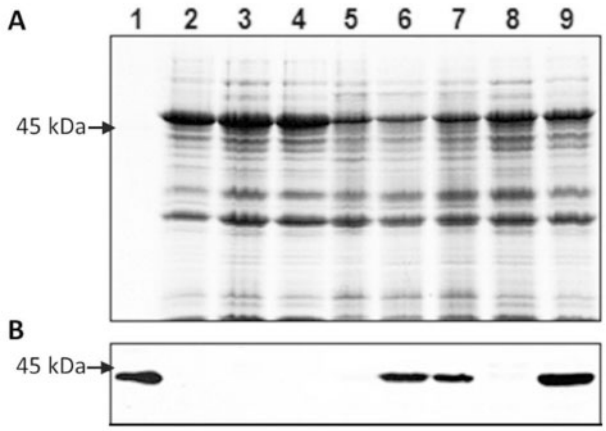

Fig. 5 Immunoblotting after sodium dodecyl sulfate polyacrylamide gel electrophoresis (SDS-PAGE) of protein extracts from various *A. thaliana* (Col-0) lines transformed with *35S-PcOKS*. (A) SDS-PAGE of affinity-purified PcOKS protein (lane 1, 0.02 μg) and crude protein extracts from seedlings of eight *A. thaliana* (Col-0) lines (20 μg each); (B) corresponding protein blot incubated with antibodies raised against His_6-PcOKS. 1, His_6-PcOKS produced in *E. coli*; 2, wild-type (untransformed) *A. thaliana* (Col-0); 3, control plant (transformed with the *NPT II* gene only); 4–9, *A. thaliana* lines transformed with *35S-PcOKS*, three of which (6, 7, 9) contain PcOKS protein.

of control plants. This extent of inhibition was similar to the effect of *35S-PcOKS* expression in transgenic *A. thaliana* lines.

PcOKS is located in pericycle cells of *Polygonum cuspidatum*

To gain more insight into the role of PcOKS in *P. cuspidatum* plants, the spatial distribution of the enzyme was analyzed by immunoblotting after SDS-PAGE and immunohistochemistry. For immunoblotting, crude protein extracts were prepared from various organs of *P. cuspidatum*, separated by SDS-PAGE and transferred to a nitrocellulose membrane (**Supplementary Fig. S7**). Subsequent incubation with His_6-PcOKS antibodies revealed that PcOKS is most abundant in roots, less abundant in the rhizome and young leaves and faintly present in petioles, whereas no immunoreaction occurred with protein from stem and mature leaves (**Fig. 8A**).

The spatial distribution of PcOKS in roots of *P. cuspidatum* was studied immunohistochemically. In cross-sections, bright immunofluorescence was observed in individual cells of the pericycle, which is the outermost cell layer of the central cylinder (**Fig. 8B, C**). Upon incubation with preimmune IgG, no specifically stained cells were detected (**Fig. 8D**). Pericycle cells were also stained in longitudinal sections (**Fig. 8E, F**). Cortex and xylem cells exhibited low background immunostaining after treatment with both anti-PcOKS and preimmune antibodies. The identity of the pericycle as the subendodermal layer was confirmed by Sudan III staining of the Casparian strip in the endodermis (**Fig. 8G**).

Discussion

The major active constituents of *P. cuspidatum* are anthranoids and stilbenes. A cDNA encoding stilbene synthase (STS), which catalyzes the biosynthesis of the stilbene skeleton, was previously isolated and characterized (Guo et al. 2013). In this study, a cDNA encoding PcOKS of *P. cuspidatum* was isolated using a homology-based cloning strategy. Although the affinity-purified enzyme, which was heterologously produced in *E. coli*, showed OKS activity in the in vitro assay, only unphysiologically folded aromatic octaketides were formed and the expected rightly cyclized products, i.e. atrochrysone and/or emodin anthrone, were not detected. However, expression of the PcOKS ORF in *A. thaliana* resulted in the formation of emodin in roots of transgenic lines. In addition, the transgenic plants showed a phenotype of strongly reduced root growth, which resembled the appearance caused by exogenous addition of emodin to the growth medium of wild-type *A. thaliana*. Our results indicate that (i) PcOKS is involved in the biosynthesis of emodin and (ii) *A. thaliana* as a heterologous host, unlike *E. coli*, is capable of forming a physiological octaketide derivative. Interestingly, transient expression in *Nicotiana benthamiana* of the ORF that encodes *A. arborescens* OKS failed to yield emodin and related products but resulted in SEK and SEK4 formation (Andersen-Ranberg et al. 2017). The same was true for PcOKS when transiently produced in *N. benthamiana*. Thus, transgenic *A. thaliana* plants producing PcOKS provide an interesting system for elucidating the route of plant anthranoid biosynthesis.

Under in vitro conditions, affinity-purified PcOKS from *E. coli* catalyzed the condensation of eight molecules of malonyl-CoA to form incorrectly folded aromatic octaketides as main products. Compared to the in vitro activities of the recombinant OKSs from *A. arborescens* and *H. perforatum* (Abe et al. 2005a, Karppinen et al. 2008, Mizuuchi et al. 2009), PcOKS did not form SEK4. Instead, SEK4b and 6-(7-hydroxy-5-methyl-4-oxo-4*H*-chromen-2-yl)-3,5-dioxohexanoic acid were identified as major products. Both products were previously described as 'non-catalytic' cyclizations of the nascent polyketide that is released by the minimal type II PKS from *Streptomyces coelicolor*, a heterodimeric complex of ketosynthase and a chain length factor, in the absence of ketoreductase (Fu et al. 1994a, Fu et al. 1994b). The first ring of SEK4, which corresponds to C7-C12 of the octaketide, was formed by the minimal PKS. PcOKS from *E. coli* thus did not catalyze any physiological cyclization of the octaketide intermediate.

Formation of emodin by PcOKS produced in transgenic *A. thaliana* roots may be due to additional yet unknown factors, which work together with PcOKS to cyclize the linear octaketide intermediate into the physiological product atrochrysone (**Fig. 1**). Elimination of water from atrochrysone to form emodin anthrone and subsequent oxidation of this intermediate to emodin appear to be catalyzed by unspecific *A. thaliana* enzymes. Mixing affinity-purified PcOKS from *E. coli* with crude cell-free extract from wild-type *A. thaliana* roots led to the formation of the same shunt product profile as purified PcOKS alone in in vitro assays (**Supplementary Fig. S8**).

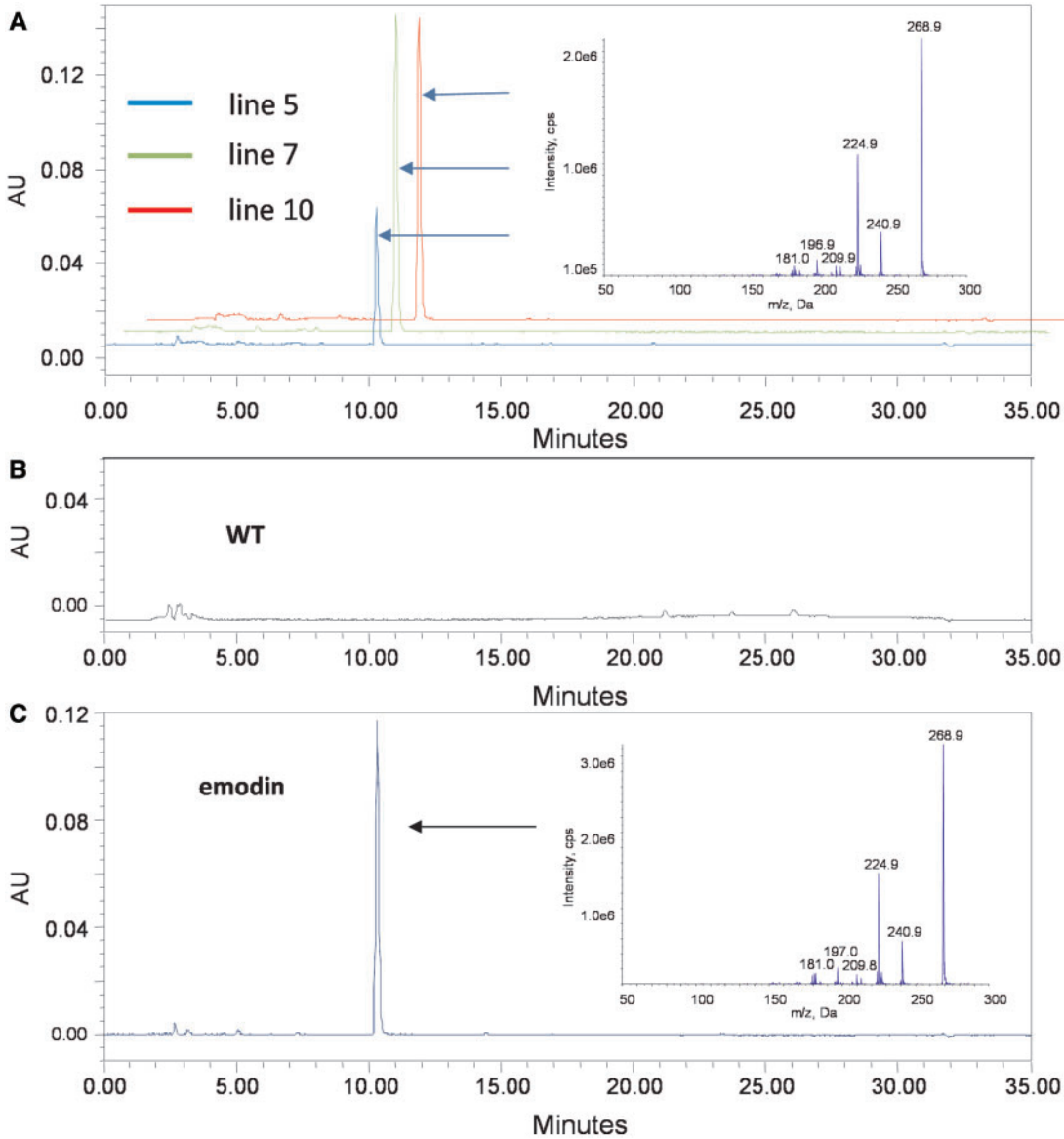

Fig. 6 Detection of emodin in ethanol (70%) extracts of transgenic *A. thaliana* (Col-0) roots. The HPLC-DAD chromatograms shown were recorded at 440 nm. At 300 nm, further components of the extracts and the internal standard (4-hydroxybiphenyl) were visible (**Supplementary Fig. S9**). Emodin was verified by ESI-MS-MS (inserts, higher resolution spectra shown in **Supplementary Fig. S11**). (A) Emodin was detected in roots of three *A. thaliana* (Col-0) lines expressing the PcOKS ORF; (B) no emodin could be detected in roots of wild-type (WT) *A. thaliana*; and (C) emodin as authentic reference compound.

These results indicate that formation of atrochysone is not simply multiple cyclization of the linear octaketide by independent octaketide cyclase(s), assuming cyclase stability upon the preparation of cell-free extract. In *A. thaliana* roots, the physiological folding of PcOKS may be assisted by chaperones and/or PcOKS may undergo posttranslational modification to achieve its final functional conformation. These processes may enable PcOKS to either form atrochrysone itself via correct cyclization of the linear octaketide or physically interact with cyclase(s), yielding an atrochrysone-forming enzyme complex. Chaperones assist protein folding, promoting the achievement of the functional conformation (Schopf et al. 2017). Posttranslational modifications, such as phosphorylation, acetylation and methylation, are crucial for controlling protein stability, localization and conformation and were shown to increase the production of properly folded soluble proteins (Kwon et al. 2006, Tokmakov et al. 2012). Conformational changes induced by posttranslational modification also affect interacting partners (Duan and Walther 2015). Previously, the formation of emodin anthrone was demonstrated using cell-free extracts from yeast extract-treated *Cassia bicapsularis* cell cultures (Abdel-Rahman et al. 2013). This was the first experimental evidence for the in vitro formation of the anthranoid scaffold by plant enzyme(s). Potentially required tailoring enzyme(s) or factor(s) obviously existed in the cell-free extract and appropriately interacted with OKS in the enzyme assay. In

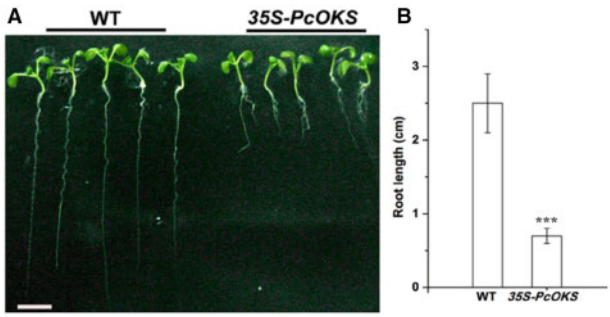

Fig. 7 Inhibition of root growth of transgenic *A. thaliana* (Col-0) plants expressing *35S-PcOKS*. (A) Morphology of seedlings expressing *35S-PcOKS* and wild-type (WT) 5 d after germination on 1/2 MS medium; (B) average root length of *35S-PcOKS* expressing and WT seedlings (three transgenic lines, five plants from each line). Bar, 1 cm. Error bars represent SD. $^{***}P < 0.001$ by Student's *t*-test.

bacteria, type I (modular type) and type II PKSs (subunit type) commonly contain additional subunits, such as cyclase, ketoreductase and aromatase, which are required for correct cyclization of linear polyketides and further modification of specifically cyclized polyketide products (Fu et al. 1994a, Fu et al. 1994b, Hertweck et al. 2004). These additional subunits cooperate with PKS to stabilize the highly reactive linear polyketide chain, thereby preventing it from nonspecific cyclizations.

Like OKS, several other plant-specific type III PKSs that were produced in *E. coli* did not form in vitro the expected products that are synthesized in the original plants. These enzymes include hexaketide synthase of *P. indica* (PiHKS, Springob et al. 2007), heptaketide synthase of *D. lusitanicum* (DlHKS, Jindaprasert et al. 2008), WtPKS1 of *Wachendorfia thyrsiflora* (Brand et al. 2006), and HsPKS1of *Huperzia serrata* (Wanibuchi et al. 2007). Given the increasing number of recombinant plant

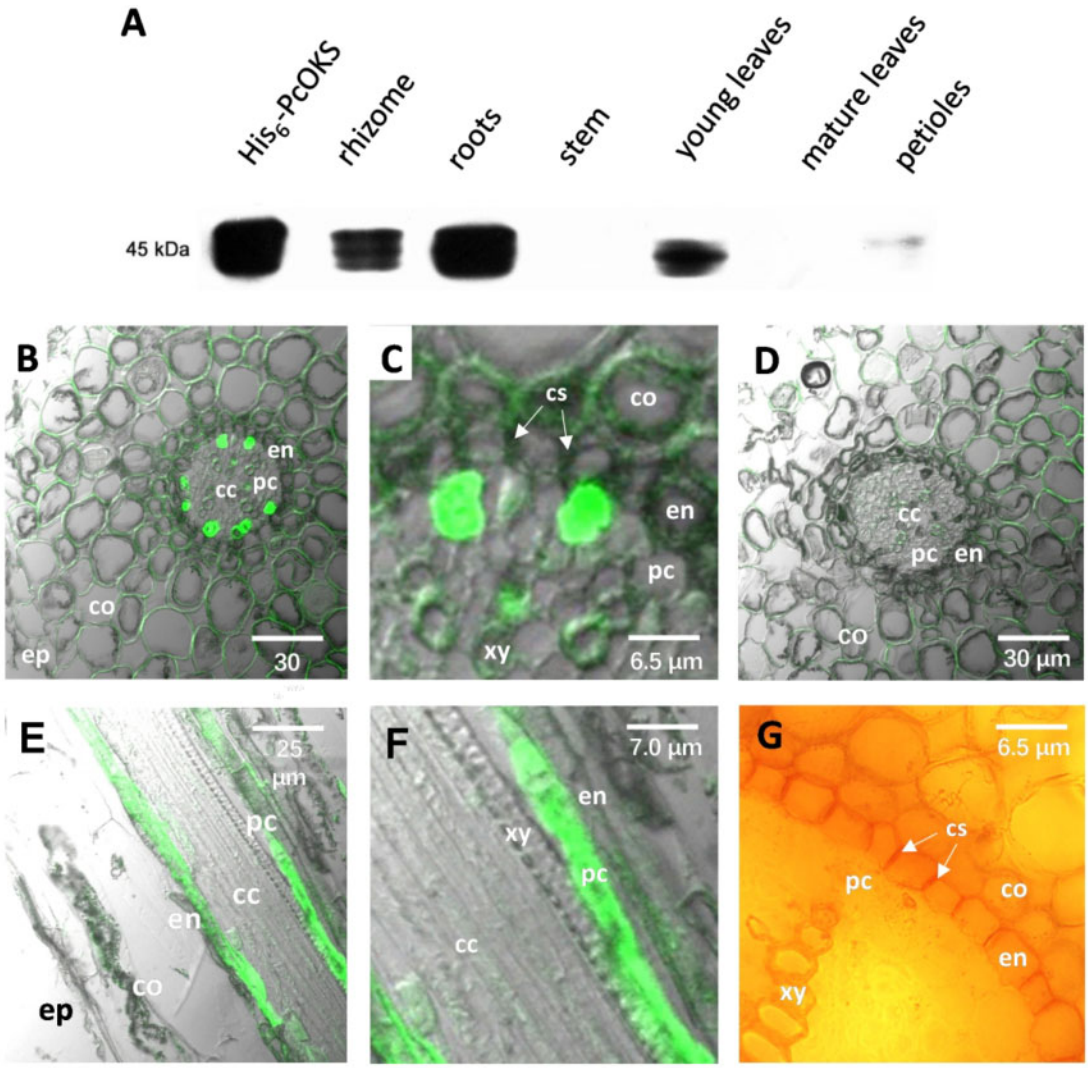

Fig. 8 Immunochemical detection of PcOKS in *Polygonum cuspidatum*. (A) Immunoblotting after sodium dodecyl sulfate polyacrylamide gel electrophoresis (SDS-PAGE) of crude protein extracts from various organs. Affinity-purified His_6-PcOKS produced in *E. coli* was used as a reference. (B–F) Immunofluorescence localization of PcOKS in roots. Transverse (B and C) and longitudinal sections (E and F) were incubated with anti-PcOKS IgG, followed by treatment with a secondary antibody coupled to green-fluorescent FITC. Incubations with preimmune IgG served as control (D). Cross-section stained with Sudan III to confirm the location of the pericycle (G). cc, central cylinder; co, cortex; cs, casparian strip; en, endodermis; ep, epidermis; pc, pericycle; xy, xylem.

type III PKSs that are known to form only unphysiological products, accessory proteins like polyketide cyclases and ketoreductases seem to play an important role in the biosynthesis of plant polyketides. A cDNA for the first polyketide cyclase of plant origin, olivetolic acid cyclase (OAC), was isolated from the medicinal plant *C. sativa* and characterized (Gagne et al. 2012). In the presence of this cyclase, the involved tetraketide synthase forms olivetolic acid, which is the key intermediate in the cannabinoid biosynthetic pathway, rather than olivetol and α-pyrones as shunt products (Taura et al. 2009, Gagne et al. 2012). The cyclase is a dimeric $\alpha+\beta$ barrel (DABB) protein that is structurally similar to polyketide cyclases from *Streptomyces* species (Thompson et al. 2004). Noteworthy, OAC works physically independent of tetraketide synthase, which appears to differ from the interaction of PcOKS and the unknown enzyme(s)/factor(s) in *A. thaliana* roots.

Interestingly, roots and rhizome are the major sites of anthranoid accumulation in *P. cuspidatum* (Liu and Hu 2001, Liu et al. 2015). Our immunochemical experiments revealed that the PcOKS protein is most abundant in these underground organs. In roots, PcOKS was present in individual cells of the pericycle, which is the outermost cell layer of the central cylinder. It is tempting to speculate that anthranoids formed in the pericycle are translocated via the adjacent vascular tissue to the aerial organs. In some polygonaceous species, such as *Rheum emodi*, anthranoids were also detected in leaves (Pandith et al. 2014). In scopolamine producing *Atropa belladonna* and *Hyoscyamus niger*, putrescine *N*-methyltransferase and hyoscyamine 6*ß*-hydroxylase, which catalyze the first and last biosynthetic steps, respectively, were localized to the pericycle, mainly to the cells adjacent to the primary xylem poles (Hashimoto et al. 1991, Kanegae et al. 1994, Suzuki et al. 1999a, Suzuki et al. 1999b). The xylem was reported to translocate tropane alkaloids, such as scopolamine, from the roots to the shoot (Neumann 1985). By contrast, the phloem is used to translocate pyrrolizidine alkaloids in *Senecio vernalis* (Hartmann et al. 1989). Homospermidine synthase, which catalyzes the first committed step in their biosynthesis, is present in distinct groups of endodermis and neighboring cortex cells located opposite to the phloem (Moll et al. 2012). In *Thalictrum flavum*, accumulation of benzylisoquinoline alkaloids is restricted to pericycle and endodermis cells and the transcripts of all genes involved in this biosynthesis were localized to the pericycle and adjacent cortical cells (Samanani et al. 2002, Samanani et al. 2005). Whether *P. cuspidatum* may use the xylem or the phloem to translocate anthranoids remains to be studied.

Materials and Methods

Plant material and reagents

Polygonum cuspidatum Sieb. et Zucc. was cultivated in the Beijing Botanical Garden and the greenhouse of the Institute of Botany, Chinese Academy of Sciences, Beijing, China. *Arabidopsis thaliana* ecotype Columbia (Col-0) was used for heterologous expression of *PcOKS*. Chemicals were of analytical grade and purchased from Fluka (Shanghai, China) and Sigma-Aldrich (Beijing, China). HPLC-grade solvents were purchased from Carl Roth (Karlsruhe, Germany). [2-^{14}C]Malonyl-CoA (55.2 mCi mmol^{-1}) was obtained from Hartmann Analytic (Braunschweig, Germany). Malonyl-CoA and acetyl-CoA were purchased from Sigma (St. Louis, MO, USA).

Molecular cloning of a PcOKS cDNA

Extraction of total RNA from roots of *P. cuspidatum* and reverse transcription were carried out as described before (Guo et al. 2013). The core fragment of the PcOKS cDNA was amplified using degenerate primers derived from conserved regions of plant type III PKSs, Dp-S and Dp-A (**Supplementary Table S1**), and the PCR program 1 (**Supplementary Table S2**). The PCR product was gel-purified and subcloned into the pMD18-T vector (TaKaRa, Beijing, China) for sequencing.

The 3′ and 5′ ends of the PcOKS cDNA were obtained by rapid amplification of cDNA ends (RACE). Two 3′ end gene-specific primers, GSP3-1 and GSP3-2, and three 5′ end gene-specific primers, GSP5-1, GSP5-2 and GSP5-3, were designed based on the core sequence obtained. The PCR program 2 was used for amplification.

The ORF of the PcOKS cDNA was amplified using the primers PcOKS-S and PcOKS-A and the PCR program 3. The amplified DNA was digested with *Nde*I and *Xho*I, subcloned into the pMD18-T vector (TaKaRa) and sequenced.

Genomic DNA extraction from young leaves of *P. cuspidatum* was carried out as described before (Guo et al. 2011). A full-length gene was amplified using the gene-specific primers PcOKS gene-S and PcOKS gene-A and the PCR program 4. The gel-purified PCR product was ligated into the pMD18-T vector (TaKaRa) and sequenced.

Heterologous expression and purification of the recombinant protein

The pMD18-T vector containing the ORF of PcOKS was digested with *Nde*I and *Xho*I. The target fragment was collected and cloned into the *Nde*I and *Xho*I sites of pET-30a (+) (Novagen, Darmstadt, Germany). The recombinant vector pET-30a (+) containing the ORF of PcOKS was transformed into the *E. coli* strain BL21-Rosetta (DE3) (TransGen, Beijing, China) and cultured at 220 rpm and 37°C in 100 ml of Luria-Bertani medium containing kanamycin (30 μg ml^{-1}). When the OD_{600} of the cultures reached 0.6–0.8, 0.5 mM isopropyl-D-1-thiogalacto-pyranoside (IPTG) was added and the cultures were incubated for another 8 h at 25°C.

The cells were harvested by centrifugation, resuspended in 3 ml of 0.1 M lysis buffer (pH 7.5) and sonified on ice for 5 min at 50% pulses using an Ultrasonic Crasher (Ningbo Scientz Biotechnology, China). The homogenate was centrifuged for 10 min at 18,894 × *g* and 4°C. The supernatant was passed through a column of Ni-NTA His-Bin Resin (Novagen) containing Ni^{2+} as an affinity ligand because the recombinant PcOKS protein contained a hexahistidine tag at the C terminus. After washing with 0.1 M PBS buffer pH 7.5 containing 0.5 M NaCl and 40 mM imidazole, the recombinant protein was eluted with 0.1 M PBS buffer, pH 7.5, containing 400 mM imidazole. For long-term storage, the buffer was changed to 0.1 M PBS buffer, pH 7.5, using a PD-10 column (Amersham Pharmacia Biotech, Uppsala, Sweden). The final PcOKS solution was divided into 100 μl aliquots and stored at −80°C. The efficiency of purification was monitored by SDS-PAGE. Protein concentrations were determined by the Bradford method (Bradford 1976) using bovine serum albumin as the standard.

Enzyme assays

The standard assay contained 64 μM acetyl-CoA, 240 μM malonyl-CoA and 2 μg purified enzyme protein in a final volume of 250 μl, filled up with 0.1 M potassium phosphate buffer, pH 7.0. For the radioactive assay containing [2-^{14}C] malonyl-CoA (3.1 kBq), the reaction volume and the protein amount were reduced to 125 μl and 1 μg, respectively. The substrate concentrations were the same. After incubation at 37°C for 30 min, the reaction was stopped by adding 1/10 volume of 20% HCl. The assay was extracted twice with the same volume of ethyl acetate. The organic phases were combined and dried under an air steam. The residue was dissolved in 50 μl methanol (50%) for HPLC analysis. For enzyme characterization, pH values ranged from 5 to 10, temperatures from 20 to 65°C, incubation times from 2.5 to 120 min and the enzyme amount from 0.5 to 32 μg per assay. Kinetic constants were determined using seven concentrations of malonyl-CoA covering the range of 0.2- to 3.0-fold K_m. The assays contained 2 μg of protein and the incubation time was reduced to 10 min at

45°C. All the characterization studies were carried out in triplicates. The K_m value was determined by the Hanes method using the Hyper 32 software for evaluation (http://homepage.ntlworld.com/john.easterby/software.html).

Analytic procedures

HPLC was carried out on a VWR-Hitachi LaChrom Elite system (pump L-2130, autosampler L-2200, diode array detector L-2455), equipped with a Symmetry column (C_8, 4.6 mm × 150 mm, 3.5 μm; Waters, Eschborn, Germany). The solvents used were 0.1% formic acid in water (A) and acetonitrile (B). The gradient included 2 min at 5% B, a linear increase to 30% B in 20 min, followed by washing at 95% B for 4 min and equilibration to 5% B for 8 min. The flow rate was 0.5 ml min^{-1} and UV spectra were recorded from 200 to 500 nm. For emodin detection, the gradient was 2 min at 50% B, a linear increase to 90% in 20 min. The flow rate was 0.7 ml min^{-1}.

For the analysis of radiolabeled products, an Agilent 1200 series HPLC system (HP 1200 binary pump, HP 1200 autosampler, HP 1200 variable wavelength detector) was complemented with a Ramona Star 2 radiodetector (Elysia-raytest, Straubenhardt, Germany) and operated by the Gina Star 4.06 software on Windows XP. A Lichrospher 100 RP C_{18} (150 mm × 4.6 mm, 5 μm; WICOM, Heppenheim, Germany) was used for separation. The mobile phase consisted of 0.1% formic acid (A) and methanol (B) using the following gradient: 20% B for 2 min and then 20–50% B in 15 min at a flow rate of 1 ml min^{-1}.

For ESI-MS characterization, the products of 20 standard incubations were pooled and purified by HPLC. The individual fractions were directly infused into the mass spectrometer (3200 QTrap; Applied Biosystems/MDS SCIEX, Darmstadt, Germany), equipped with an electrospray ionization interface (Turbo V). The integrated syringe pump of the 3200 QTrap instrument (Syringe; 1,000 ml, i.d. 2.3 mm; Hamilton, Nevada, USA) was used at a flow rate of 10 μl min^{-1}. Tandem mass spectrometry (MS/MS) was operated in the negative mode with a source voltage and declustering potential of 4.5 kV and 76 V, respectively. Nitrogen gas was used for nebulization, with the curtain gas, gas 1 and gas 2 settings at 10, 14 and 0, respectively. The pseudo molecular ion peaks $[M-H]^-$ of corresponding products were further analyzed by MS/MS experiments in the enhanced product ion mode of the instrument using nitrogen gas for collision-induced dissociation at the high-level setting. The collision energy was −50 to −30 eV, individually optimized for each compound. Data acquisition and processing were performed using the Analyst software (version 1.64.2; Applied Biosystems/MDS SCIEX).

Homology modeling

Homology modeling was performed in the Phyre2 web portal (http://www.sbg.bio.ic.ac.uk/phyre2/html/page.cgi?id=index; Kelley et al. 2015). The default settings indicated on the website were used. To calculate the cavity size, the homology modeling results from Phyre2 were entered into the website CASTp3 (http://sts.bioe.uic.edu/castp/index.html?4jii; Tian et al. 2018). The final results of CASTp3 were analyzed using the program UCSF Chimera (version 1.13.1; Pettersen et al. 2004).

Phylogenetic analysis

A total of 71 selected plant type III PKS sequences with clear functional information were used for constructing a phylogenetic tree by the neighbor-joining method in MEGA7 (Saitou and Nei 1987, Kumar et al. 2016). The percentages of replicate trees in which the associated taxa clustered together in the bootstrap test (500 replicates) are shown next to the branches (Felsenstein 1985). The evolutionary distances were computed using the Dayhoff matrix-based method (Schwarz and Dayhoff 1979). The final dataset included a total of 474 positions.

Raising antibodies and immunoblotting after SDS-PAGE

The ORF of the PcOKS cDNA was expressed in *E. coli* and the recombinant protein was purified using a hexahistidine tag. An antiserum against His_6-PcOKS was generated in rabbits (Laboratory Animal Center, Institute of Genetics and Developmental Biology, Chinese Academy of Sciences, Beijing, China). The IgG fraction of the antiserum was isolated by affinity chromatography on a HiTrap Protein A HP column (1 ml; GE Healthcare) according to the manufacturer's instructions. Aliquots of the IgG fraction were stored at −80°C in PBS buffer.

Protein was extracted from young leaves, mature leaves, petioles, stems, roots and rhizomes of *P. cuspidaum* and seedling of *A. thaliana* using 100 mM potassium phosphate buffer pH 7.5 containing 10 mM DTT. The protein concentration was determined according to the Bradford method (Bradford 1976) using bovine serum albumin as the standard. The protein extracts (20 μg) were separated on a 10% SDS gel and the band patterns were transferred on a nitrocellulose membrane (Millipore, Boston, MA, USA). The membrane was blocked with 5% (w/v) defatted milk powder in a blocking buffer (20 mmol l^{-1} Tris-HCl, pH 7.4, 0.8% NaCl and 0.05% Tween 20) at 25°C for 1 h. It then was incubated with anti-His_6-PcOKS IgG at a 1:5,000 dilution with tris-buffered saline (TBS) buffer (20 mmol l^{-1} Tris-HCl, pH 7.4, 0.8% NaCl, 0.05% Tween 20) for 3 h at 25°C. After washing 3× 10 min with TBS buffer, the membrane was incubated with peroxidase-conjugated AffiniPure Goat Anti-Rabbit IgG (Xinjingke, Beijing, China) at a 1:2,000 dilution in TBS buffer and 25°C for 1 h. Binding of the secondary antibody was visualized using SuperSignal West Pico Chemiluminescent Substrate (Pierce Chemical Co., Rockford, IL, USA).

Immunohistochemical localization of PcOKS

Roots of *P. cuspidatum* were rinsed with tap water, dried on filter paper and cut into 0.5 cm × 0.5 cm slices, which were immediately immersed in a fixative containing 4% paraformaldehyde in 100 mM PBS (pH 7.2) for 6 h at 25°C. After dehydration, samples were embedded in paraffin wax and cut into 10-μm sections using a Leica RM 2235 microtome (Leica, Germany). Sections were placed on poly-L-lysine-coated slides and stretched by the addition of a small drop of water. After de-embedding and rehydration, the sections were used for immunohistochemical localization. The slides were blocked with 5% defatted milk powder in a blocking solution (20 mmol l^{-1} Tris-HCl, pH 7.4, 0.8% NaCl, 0.05% Tween 20) for 20 min at 37°C and then incubated for 1 h at 25°C with anti-His_6-PcOKS IgG diluted 1:500 in blocking solution with 3% defatted milk powder. After several washings with TBS buffer, the slides were incubated for 1 h at 25°C with the fluorescein isothiocyanate (FITC)-conjugated secondary antibody, diluted 1:2,000 in blocking solution with 3% defatted milk powder. The sections were viewed under a laser scanning microscope (Zeiss LSM 510META).

Heterologous expression of *PcOKS* in *Arabidopsis thaliana*

The *PcOKS* ORF was amplified by PCR using sense (5′-GCA CTC GAG TCA CAG AAT TGG AAC ACT-3′; *Xho*I site underlined) and antisense primers (5′-GTA GGA TCC ATG GCG AAT GTA CTG CA-3′; *Bam*HI site underlined). It then was inserted into the *Xho*I and *Bam*HI sites of the plant expression vector pBI121 to generate pBI::*PcOKS*. The *Xho*I site immediately behind the GUS ORF in pBI121 was created using a PCR-based mutagenesis approach (Shimada 1996). The resulting pBI::*PcOKS* plant expression vector was transferred into the *A. tumefaciens* strain GV3101 for *A. thaliana* transformation, which was performed by the floral dip method (Clough and Bent 1998). Seeds of *A. thaliana* were collected and germinated on 1/2× MS medium containing 40 mg l^{-1} kanamycin to select for transgenic plants. The selected kanamycin-resistant seedlings (T1 generation) were transferred into the soil. *Arabidopsis thaliana* materials were grown on half-strength MS medium at 22°C under standard long-day conditions (16-h light, 8-h dark).

Three transgenic *A. thaliana* lines (Supplementary Table S3) were used for studying product profiles. *Arabidopsis thaliana* plants (both transgenic and wild type) were grown in pots with soil for 8 weeks in controlled environment chambers (Percival) at 22°C, 60–70% relative humidity and 300 μmol m^{-2} s^{-1} photosynthetically active radiation (photoperiod 16 h). Because of the small amounts of root material, roots of 2–4 plants of each transgenic line were combined. The roots and in addition the shoots were lyophilized and ground to a fine powder using a mixer mill (Mixer Mill MM400, Retsch, Haan, Germany) at 29 Hz for 1 min. The powder was extracted with 1 ml ethanol (70%) containing 50 μg of 4-hydroxybiphenyl as internal standard and the extract was dried under a nitrogen stream. The residue was redissolved in 100 μl of dimethyl sulfoxide and analyzed by HPLC-DAD. The emodin peak was collected and analyzed by ESI-MS, as described above. The emodin amount was quantified using an emodin calibration curve prepared in the HPLC-DAD system (Supplementary Fig. S10).

Supplementary Data

Supplementary data are available at PCP online.

Funding

The National Natural Science Foundation of China (NSFC) (Grant Nos. 61972374 and 61672489 to H.W.) and the Deutsche Forschungsgemeinschaft (Grant No. BE 1174/14-1 to L.B.).

Disclosures

The authors have no conflict of interest to declare.

References

Andersen-Ranberg, J., Kongstad, K.T., Nafisi, M., Staerk, D., Okkels, F.T., Mortensen, U.H., et al. (2017) Synthesis of C-glucosylated octaketide anthraquinones in *Nicotiana benthamiana* by using a multispecies-based biosynthetic pathway. *ChemBioChem* 18: 1893–1897.

Abdel-Rahman, I.A., Beuerle, T., Ernst, L., Abdel-Baky, A.M., Desoky, E.E.-D.K., Ahmed, A.S., et al. (2013) In vitro formation of the anthranoid scaffold by cell-free extracts from yeast-extract-treated *Cassia bicapsularis* cell cultures. *Phytochemistry* 88: 15–24.

Abe, I. and Morita, H. (2010) Structure and function of the chalcone synthase superfamily of plant type III polyketide synthases. *Nat. Prod. Rep.* 27: 809–838.

Abe, I., Oguro, S., Utsumi, Y., Sano, Y. and Noguchi, H. (2005a) Engineered biosynthesis of plant polyketides: chain length control in an octaketide-producing plant type III polyketide synthase. *J. Am. Chem. Soc.* 127: 12709–12716.

Abe, I., Utsumi, Y., Oguro, S., Morita, H., Sano, Y. and Noguchi, H. (2005b) A plant type III polyketide synthase that produces pentaketide chromone. *J. Am. Chem. Soc.* 127: 1362–1363.

Abe, I., Utsumi, Y., Oguro, S. and Noguchi, H. (2004) The first plant type III polyketide synthase that catalyzes formation of aromatic heptaketide. *FEBS Lett.* 562: 171–176.

Abe, I., Watanabe, T., Lou, W. and Noguchi, H. (2006) Active site residues governing substrate selectivity and polyketide chain length in aloesone synthase. *FEBS J.* 273: 208–218.

Austin, M.B., Bowman, M.E., Ferrer, J.-L., Schröder, J. and Noel, J.P. (2004) An aldol switch discovered in stilbene synthases mediates cyclization specificity of type III polyketide synthases. *Chem. Biol* 11: 1179–1194.

Austin, M.B. and Noel, J.P. (2003) The chalcone synthase superfamily of type III polyketide synthases. *Nat. Prod. Rep.* 20: 79–110.

Bradford, M.M. (1976) A rapid and sensitive method for the quantitation of microgram quantities of protein utilizing the principle of protein-dye binding. *Anal. Biochem.* 72: 248–254.

Brand, S., Hölscher, D., Schierhorn, A., Svatoš, A., Schröder, J. and Schneider, B. (2006) A type III polyketide synthase from *Wachendorfia thyrsiflora* and its role in diarylheptanoid and phenylphenalenone biosynthesis. *Planta* 224: 413–428.

Clough, S.J. and Bent, A.F. (1998) Floral dip: a simplified method for *Agrobacterium*-mediated transformation of *Arabidopsis thaliana*. *Plant J.* 16: 735–743.

Dewick, P.M. (2009) *Medicinal Natural Products, A Biosynthetic Approach*, 3rd edn. Wiley, Chichester, UK.

Dommanget, F., Cavaillé, P., Evette, A. and Martin, F. (2016) Asian knotweeds-an example of a raising threat? *In Introduced Tree Species in European Forests: Opportunities and Challenges*, pp. 202–211. European Forest Institute, Freiburg, Germany.

Duan, G. and Walther, D. (2015) The roles of post-translational modifications in the context of protein interaction networks. *PLoS Comput. Biol.* 11: e1004049.

Eckermann, S., Schröder, G., Schmidt, J., Strack, D., Edrada, R.A., Helariutta, Y., et al. (1998) New pathway to polyketides in plants. *Nature* 396: 387–390.

Editorial Committee of Chinese Pharmacopoeia (1977) *Chinese Pharmacopoeia, 1977*. p. 340. Medical Science and Technology Press, Beijing, China.

Editorial Committee of Chinese Pharmacopoeia (2015) *Chinese Pharmacopoeia, 2010*. pp. 208–209. Medical Science and Technology Press, Beijing, China.

Felsenstein, J. (1985) Confidence limits on phylogenies: an approach using the bootstrap. *Evolution* 39: 783–791.

Ferrer, J.L., Jez, J.M., Bowman, M.E., Dixon, R.A. and Noel, J.P. (1999) Structure of chalcone synthase and the molecular basis of plant polyketide biosynthesis. *Nat. Struct. Biol.* 6: 775–784.

Fu, H., Ebert-Khosla, S., Hopwood, D.A. and Khosla, C. (1994a) Engineered biosynthesis of novel polyketides: dissection of the catalytic specificity of the act ketoreductase. *J. Am. Chem. Soc.* 116: 4166–4170.

Fu, H., Hopwood, D.A. and Khosla, C. (1994b) Engineered biosynthesis of novel polyketides: evidence for temporal, but not regiospecific, control of cyclization of an aromatic polyketide precursor. *Chem. Biol.* 1: 205–210.

Gagne, S.J., Stout, J.M., Liu, E., Boubakir, Z., Clark, S.M. and Page, J.E. (2012) Identification of olivetolic acid cyclase from *Cannabis sativa* reveals a unique catalytic route to plant polyketides. *Proc. Natl. Acad. Sci. USA* 109: 12811–12816.

Gao, F., Liu, W., Guo, Q., Bai, Y., Yang, H. and Chen, H. (2017) Physcion blocks cell cycle and induces apoptosis in human B cell precursor acute lymphoblastic leukemia cells by downregulating HOXA5. *Biomed. Pharmacother.* 94: 850–857.

Guo, Y., Ma, L., Ji, Y., Pu, G., Liu, B., Du, Z., et al. (2011) Isolation of the 5′-end of plant genes from genomic DNA by TATA-box-based degenerate primers. *Mol. Biotechnol.* 47: 152–156.

Guo, Y.W., Guo, H.L., Li, X., Huang, L.L., Zhang, B.N., Pang, X.B., et al. (2013) Two type III polyketide synthases from *Polygonum cuspidatum*: gene structure, evolutionary route and metabolites. *Plant Biotechnol. Rep.* 7: 371–381.

Hartmann, T., Ehmke, A., Eilert, U., von Borstel, K. and Theuring, C. (1989) Sites of synthesis, translocation and accumulation of pyrrolizidine alkaloid N-oxides in *Senecio vulgaris* L. *Planta* 177: 98–107.

Hashimoto, T., Hayashi, A., Amano, Y., Kohno, J., Iwanari, H., Usuda, S., et al. (1991) Hyoscyamine 6 beta-hydroxylase, an enzyme involved in tropane alkaloid biosynthesis, is localized at the pericycle of the root. *J. Biol. Chem.* 266: 4648–4653.

Hertweck, C., Xiang, L., Kalaitzis, J.A., Cheng, Q., Palzer, M. and Moore, B.S. (2004) Context-dependent behavior of the enterocin iterative polyketide synthase: a new model for ketoreduction. *Chem. Biol.* 11: 461–468.

Jayasuriya, H., Koonchanok, N.M., Geahlen, R.L., McLaughlin, J.L. and Chang, C.J. (1992) Emodin, a protein tyrosine kinase inhibitor from *Polygonum cuspidatum*. *J. Nat. Prod.* 55: 696–698.

Jez, J.M., Austin, M.B., Ferrer, J.L., Bowman, M.E., Schröder, J. and Noel, J.P. (2000) Structural control of polyketide formation in plant-specific polyketide synthases. *Chem. Biol.* 7: 919–930.

Jindaprasert, A., Springob, K., Schmidt, J., De-Eknamkul, W. and Kutchan, T.M. (2008) Pyrone polyketides synthesized by a type III polyketide synthase from *Drosophyllum lusitanicum*. *Phytochemistry* 69: 3043–3053.

Kanegae, T., Kajiya, H., Amano, Y., Hashimoto, T. and Yamada, Y. (1994) Species-dependent expression of the hyoscyamine 6 [beta]-hydroxylase gene in the pericycle. *Plant Physiol.* 105: 483–490.

Karppinen, K., Hokkanen, J., Mattila, S., Neubauer, P. and Hohtola, A. (2008) Octaketide-producing type III polyketide synthase from *Hypericum*

perforatum is expressed in dark glands accumulating hypericins. *FEBS J.* 275: 4329–4342.

Kelley, L.A., Mezulis, S., Yates, C.M., Wass, M.N. and Sternberg, M.J. (2015) The Phyre2 web portal for protein modeling, prediction and analysis. *Nat. Protoc.* 10: 845–858.

Kumar, S., Stecher, G. and Tamura, K. (2016) MEGA7: molecular evolutionary genetics analysis version 7.0 for bigger datasets. *Mol. Biol. Evol.* 33: 1870–1874.

Kwon, S.J., Choi, E.Y., Choi, Y.J., Ahn, J.H. and Park, O.K. (2006) Proteomics studies of post-translational modifications in plants. *J. Exp. Bot.* 57: 1547–1551.

Li, C., Zhang, Y., Zheng, L., Zheng, Y., Huang, P., Xiao, X., et al. (2019) Assembly and annotation of a draft genome of the medicinal plant *Polygonum cuspidatum*. *Front. Plant Sci.* 10: 1274.

Liu, W. and Hu, Z. (2001) Histochemical localization and quantitative analysis of anthraquinones in rhizome of *Polygonum cuspidatum*. *Acta Biol. Exp. Sin.* 34: 235–241.

Liu, Y., Wang, J., Chu, S., Cheng, M. and Fang, C. (2015) Distribution laws of 5 compounds in rhizome and root of *Polygonum cuspidate*. *Zhongguo Zhong Yao Za Zhi* 40: 4834–4839.

Ma, L.Q., Guo, Y.W., Gao, D.Y., Ma, D.M., Wang, Y.N., Li, G.F., et al. (2009a) Identification of a *Polygonum cuspidatum* three-intron gene encoding a type III polyketide synthase producing both naringenin and *p*-hydroxybenzalacetone. *Planta* 229: 1077–1086.

Ma, L.Q., Pang, X.B., Shen, H.Y., Pu, G.B., Wang, H.H., Lei, C.Y., et al. (2009b) A novel type III polyketide synthase encoded by a three-intron gene from *Polygonum cuspidatum*. *Planta* 229: 457–469.

Mizuuchi, Y., Shi, S.P., Wanibuchi, K., Kojima, A., Morita, H., Noguchi, H., et al. (2009) Novel type III polyketide synthases from *Aloe arborescens*. *FEBS J.* 276: 2391–2401.

Moll, S., Anke, S., Kahmann, U., Hänsch, R., Hartmann, T. and Ober, D. (2002) Cell-specific expression of homospermidine synthase, the entry enzyme of the pyrrolizidine alkaloid pathway in *Senecio vernalis*, in comparison with its ancestor, deoxyhypusine synthase. *Plant Physiol.* 130: 47–57.

Murrell, C., Gerber, E., Krebs, C., Parepa, M., Schaffner, U. and Bossdorf, O. (2011) Invasive knotweed affects native plants through allelopathy. *Am. J. Bot.* 98: 38–43.

Neumann, D. (1985) Storage of alkaloids. *In Biochemistry of Alkaloids*. Edited by Mothes, K., Schütte, H.R. and Luckner, M. pp. 49–55. VCH, Weilheim, Germany.

Olsen, B.B., Bjørling-Poulsen, M. and Guerra, B. (2007) Emodin negatively affects the phosphoinositide 3-kinase/AKT signalling pathway: a study on its mechanism of action. *Int. J. Biochem. Cell Biol.* 39: 227–237.

Pandith, S.A., Hussain, A., Bhat, W.W., Dhar, N., Qazi, A.K., Rana, S., et al. (2014) Evaluation of anthraquinones from Himalayan rhubarb (*Rheum emodi* Wall. ex Meissn.) as antiproliferative agents. *S. Afr. J. Bot.* 95: 1–8.

Pettersen, E.F., Goddard, T.D., Huang, C.C., Couch, G.S., Greenblatt, D.M., Meng, E.C., et al. (2004) UCSF Chimera—a visualization system for exploratory research and analysis. *J. Comput. Chem.* 25: 1605–1612.

Peng, W., Qin, R., Li, X. and Zhou, H. (2013) Botany, phytochemistry, pharmacology, and potential application of *Polygonum cuspidatum* Sieb. et Zucc.: a review. *J. Ethnopharmacol.* 148: 729–745.

Ritz, R., Scheidle, C., Noell, S., Roser, F., Schenk, M., Dietz, K., et al. (2012) In vitro comparison of hypericin and 5-aminolevulinic acid-derived protoporphyrin IX for photodynamic inactivation of medulloblastoma cells. *PLoS One* 7: e51974.

Saitou, N. and Nei, M. (1987) The neighbor-joining method: a new method for reconstructing phylogenetic trees. *Mol. Biol. Evol.* 4: 406–425.

Samanani, N., Park, S.-U. and Facchini, P.J. (2005) Cell type-specific localization of transcripts encoding nine consecutive enzymes involved in protoberberine alkaloid biosynthesis. *Plant Cell* 17: 915–926.

Samanani, N., Yeung, E.C. and Facchini, P.J. (2002) Cell type-specific protoberberine alkaloid accumulation in *Thalictrum flavum*. *J. Plant Physiol.* 159: 1189–1196.

Schopf, F.H., Biebl, M.M. and Buchner, J. (2017) The HSP90 chaperone machinery. *Nat. Rev. Mol. Cell Biol.* 18: 345–360.

Schröder, J. (1997) A family of plant-specific polyketide synthases: facts and predictions. *Trends Plant Sci.* 2: 373–378.

Schwarz, R. and Dayhoff, M. (1979) Matrices for detecting distant relationships. *In Atlas of Protein Sequences and Structure*. Edited by Dayhoff, M. pp. 353–358. National Biomedical Research Foundation, Washington, D. C., DC, USA.

Shan, B., Cai, Y.Z., Brooks, J.D. and Corke, H. (2008) Antibacterial properties of *Polygonum cuspidatum* roots and their major bioactive constituents. *Food Chem.* 109: 530–537.

Shimada, A. (1996) PCR-based site-directed mutagenesis. *In In Vitro Mutagenesis Protocols*. Edited by Trower, M.K. pp. 157–165. Springer, Heidelburg, Germany.

Springob, K., Samappito, S., Jindaprasert, A., Schmidt, J., Page, J.E., De-Eknamkul, W., et al. (2007) A polyketide synthase of *Plumbago indica* that catalyzes the formation of hexaketide pyrones. *FEBS J.* 274: 406–417.

Suzuki, K.-I., Yamada, Y. and Hashimoto, T. (1999a) Expression of *Atropa belladonna* putrescine N-methyltransferase gene in root pericycle. *Plant Cell Physiol.* 40: 289–297.

Suzuki, K.-I., Yun, D.J., Chen, X.Y., Yamada, Y. and Hashimoto, T. (1999b) An *Atropa belladonna* hyoscyamine 6β-hydroxylase gene is differentially expressed in the root pericycle and anthers. *Plant Mol. Biol.* 40: 141–152.

Taura, F., Tanaka, S., Taguchi, C., Fukamizu, T., Tanaka, H., Shoyama, Y., et al. (2009) Characterization of olivetol synthase, a polyketide synthase putatively involved in cannabinoid biosynthetic pathway. *FEBS Lett.* 583: 2061–2066.

Tokmakov, A.A., Kurotani, A., Takagi, T., Toyama, M., Shirouzu, M., Fukami, Y., et al. (2012) Multiple post-translational modifications affect heterologous protein synthesis. *J. Biol. Chem.* 287: 27106–27116.

Thompson, T.B., Katayama, K., Watanabe, K., Hutchinson, C.R. and Rayment, I. (2004) Structural and functional analysis of tetracenomycin F2 cyclase from *Streptomyces glaucescens* a type II polyketide cyclase. *J. Biol. Chem.* 279: 37956–37963.

Tian, W., Chen, C., Lei, X., Zhao, J. and Liang, J. (2018) CASTp 3.0: computed atlas of surface topography of proteins. *Nucleic Acids Res.* 46: W363–W367.

Vastano, B.C., Chen, Y., Zhu, N., Ho, C.-T., Zhou, Z. and Rosen, R.T. (2000) Isolation and identification of stilbenes in two varieties of *Polygonum cuspidatum*. *J. Agric. Food Chem.* 48: 253–256.

Wanibuchi, K., Zhang, P., Abe, T., Morita, H., Kohno, T., Chen, G., et al. (2007) An acridone-producing novel multifunctional type III polyketide synthase from *Huperzia serrata*. *FEBS J.* 274: 1073–1082.

Xiao, K., Xuan, L., Xu, Y., Bai, D. and Zhong, D. (2002) Constituents from *Polygonum cuspidatum*. *Chem. Pharm. Bull.* 50: 605–608.

Zhang, H., Li, C., Kwok, S.-T., Zhang, Q.-W. and Chan, S.W. (2013) A review of the pharmacological effects of the dried root of *Polygonum cuspidatum* (Hu Zhang) and its constituents. *Evid. Based Complement. Alternat. Med.* 2013: 1–13.